AERIAL PHOTOGRAPH OF SENDAI COAST FOR SHORELINE BEHAVIOR ANALYSIS

Eko Pradjoko[1] and Hitoshi Tanaka[1]

The shoreline analysis around the Nanakita River mouth has been performed by utilizing aerial photographs to reveal the different behavior between left and right side of the river mouth. The shoreline on left side of river mouth has been moving more dynamically than the right side. The empirical orthogonal function (EOF) method is also applied on the shoreline data to reveal the behavior of shoreline change. The first mode of variability reflects the cross-shore movement which is shown by uniform advance and retreat movement along the beach. The shoreline change around the Nanakita River mouth is dominated by the cross-shore movement which is shown by around 80% contribution of first mode. The second mode of variability depicts the longshore sediment movement which is shown by different shoreline movement between left and right side of river mouth. The longshore movement only contributes around 10% to the shoreline change around the Nanakita River mouth. The second mode also reveals the influence of river mouth to the longshore sediment transport characterized by different shoreline response between left and right side.

Keywords: aerial photograph; shoreline; river mouth; longshore sediment transport; empirical orthogonal function

INTRODUCTION

Backgound

The shoreline is one important feature in coastal area. As a border between land and sea, its behavior could become threaten for the utilization of coastal area if it moves retreat. It is known that the shoreline behavior is subjected by waves, current, and tides. The shoreline might have the long trend of advancement or retreat by the means of longshore sediment movement. Meanwhile, the river mouth is usually considered only as sediment source for the beach. However, the river discharge which is moving directly to the sea may influence the hydrodynamic condition in front of river mouth. Then it will interrupt the longshore transport in the adjacent shoreline even without the existence of jetty structure. Therefore, the investigation of shoreline behavior around river mouth is interesting to know their interaction.

Some researchers have investigated this influence of river mouth such as Dibajnia et al. (2004), Uzaki and Kuriyama (2007), and Kuroiwa et al. (2008). Most of them were based on process-based model (2DH and quasi-3D model). In this study, we analyze the influence of river mouth by using the application of Empirical Orthogonal Function (EOF) method on shoreline data around river mouth. Winant et al. (1975) applied firstly the EOF method to coastal morphology analysis by using beach profile data of Torrey Pines California. Since then the method has been used by another researches in many area. Recently, Miller and Dean (2007) applied this method by using shoreline position data of some places in USA and Australia. Many research results have shown the capability of EOF method to separate the cross-shore and longshore movement in coastal morphology. This study use that capability, especially on longshore movement result, to analyze the influence of rives mouth. The result of EOF method will be examined to reveal the influence of river mouth to the surrounding beach. The shoreline data around river mouth was extracted from aerial photographs which have been taken for 20 years.

Study Area

The Nanakita River is located at northern part of Sendai City in Miyagi Prefecture Japan. The length of river is 45 km and the basin area is 229.1 km^2. The flood discharge of 100-years return period is 1,650 m^3/s and average river discharge is about 10 m^3/s. The Nanakita River mouth is located at east side of Sendai City, facing to the Pacific Ocean at the Coast of Sendai City. The width of river mouth is varying due to the development of sand spit. The sand spit is developed during the low discharge and from right side in recent years.

The Coast of Sendai City is sandy beach and stretch about 12 km from Sendai Port at north until Natori River at south. However, the object of this study is only 1.8 km shoreline around the Nanakita River mouth. There is much utilization around that river mouth area such as living population, waste water treatment facility and Gamo Lagoon for environmental preservation. The location of study can be seen in Figure 1.

[1] Department of Civil Engineering, Tohoku University, 6-6-06 Aoba, Sendai 980-8579, Japan

The wave rose in Figure 2 is based on daily average wave data in Sendai Port from 1991 until 2009. The significant wave heights more than 1.0m are only 25% from all of data. The graph also indicates that the most incoming waves are from the south-east and east. These wave conditions generate longshore current and resulting sediment transport from south to north direction for overall coast. The Figure 2 also shows the tide condition from Sendai Port information. The tide has semi diurnal type with tidal range about 1.6m.

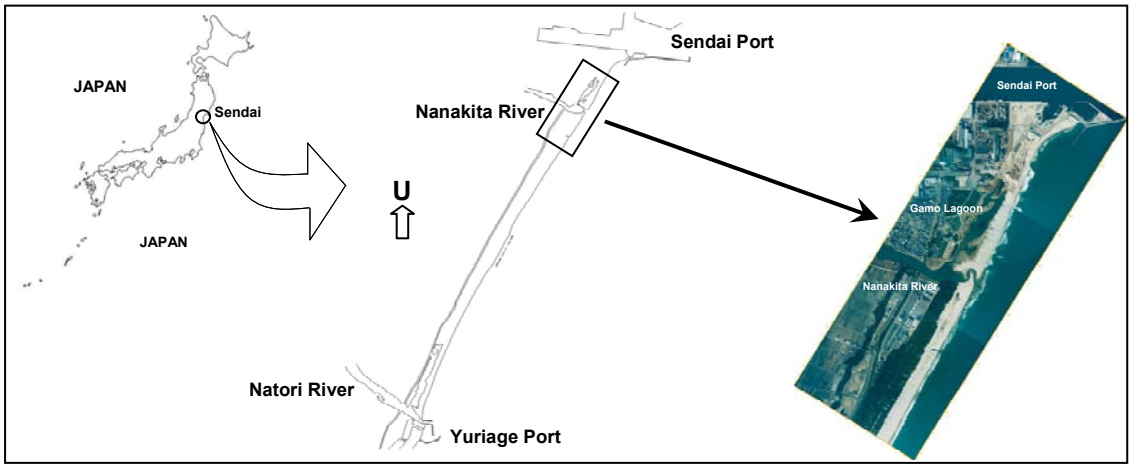

Figure 1. Study area.

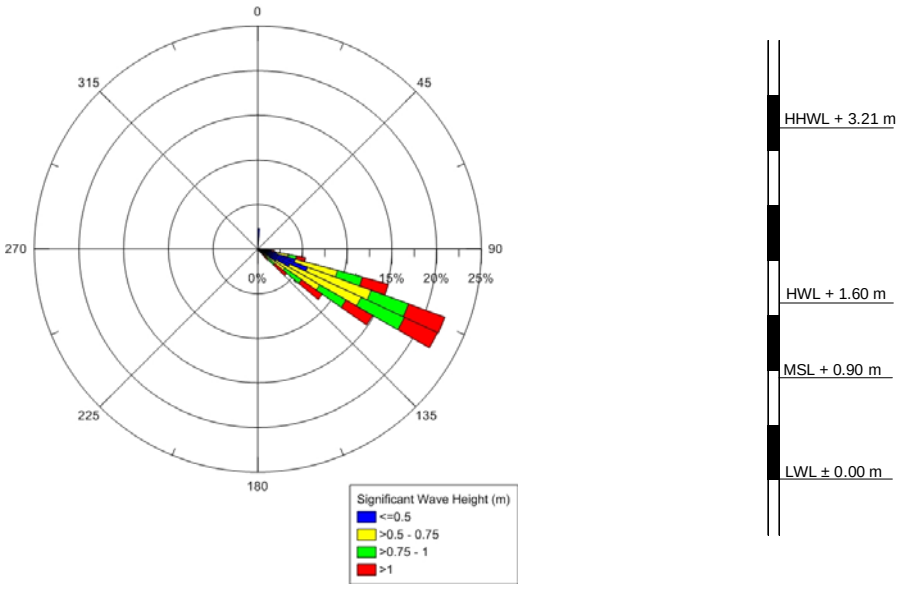

Figure 2. Offshore wave rose and tide condition.

There are some studies conducted to analyze the shoreline behavior in that area. Srivihok and Tanaka (2004) identified the influence of Sendai Port breakwater on the sand spit development in Nanakita River mouth. Kang and Tanaka (2004) analyzed the beach profile data in wider extent from Sendai Port until Natori River mouth but in limited position and time. The results showed the agreement between the EOF results and longshore transport. Khang and Tanaka (2007) identified the influence of Nanakita River mouth on the shoreline behavior around it. This study gives more effort to the identification of river mouth influence by analyzing the data of shoreline position only around river mouth and using EOF method. This study also utilizes more updated and frequently data compare with previous researches.

METHODOLOGY

Data Sources and Geo-referencing

The aerial photograph has been taken by airplane regularly since 1990 until 2009 in this study area. The images were taken monthly from 1990 until 1993 and taken every two months afterwards. Nevertheless, some year have no complete data i.e. 2008 (4 months); 2004 (3 months); 2005, 2006, 2009 (1 month). The image data covered the coastal area from Sendai Port at north end until Yuriage Port at south end as shown in Figure 1. The shoreline is centered in the image with a 60 percent overlap between adjacent images. Totally there are 19 images which cover 12 km of shoreline. The photograph is in print form with standard size 9 x 9 inches and most of them have scale of 1 : 8,000. The images were scanned in 400 dpi resolution to make it digitally. That resolution will make 1 pixel ≈ 0.50m and save in JPEG file type.

The aerial photographs have been geo-referenced by using GIS program and rectified to the coordinate system of Japanese Geodetic Datum (JGD) 2000 CS X. This coordinate system is expressed in meter distance, such as UTM system, so extracting image data will be more accurate. The 10 Ground Control Points (GCP) were collected from Japan Map within the study area. These GCP's combination give possible smallest total RMS error in rectification process which is shown by GIS program i.e. 12 pixels x 0.50m = 6.0m. This error becomes uncertainty in shoreline measurement result which will be described more clearly in uncertainty assessment section. At last the rectified image has Japan local coordinate system and the beach line oriented around 212^0 clockwise from North.

Shoreline Detection and Digitization

In the rectified image, the shoreline as proxy or feature line that will be measured have to be chosen. The method of shoreline detection and its reliability has been discussed in many papers (Crowell et al. 1991, Camfield and Morang 1996, Kraus and Rosati 1997, Boak and Turner 2005, Hanslow 2007). The High Water Line usually chosen as representation of continuous line on the image according those papers. The line is marked by the left debris along the beach face. This feature line was been usually used in many practical shoreline measurements in USA. However, this line sometime becomes difficult to identify on the image. Specially, it is happen when there is no so much debris or when the image has taken in summer session which the beach become quickly dry.

The aerial photograph was taken in instantaneous time. When the wave is calm, it is easy to detect the shoreline as border between the land and water area. But if the wave is high, the beach face will be marked by the wet-dry line which represents the wave run-up position. Therefore, this study chooses wet-dry line as proxy line and representing the wave run-up for shoreline measurement. The shoreline data will be corrected by wave run-up and tidal data for making in same position.

The shoreline detection of Sendai Coast image was being processed by using *BeachTools* extension in GIS program from CIRP project in USACE. The tool can generate automatic detection based on same pixel value of chosen line. The tool also can generate the baseline and transect for measuring shoreline position automatically. It can remove the tedium and subjectivity of extracting data by hand and allowing for much greater precision of such measurement (Hoeke et al., 2001). The total shoreline length which analyze in this study is 1,800 m. Cross-section or transect had been set up with 20 m interval. Every cross-section is approximately perpendicular to the shoreline.

The shoreline correction utilizes the wave run-up, tidal data and beach slope. Wave run-up is the maximum elevation of wave up-rush above still-water level. Hunt (1959) has presented the equations for wave run-up (R) for uniform, smooth, impermeable slopes based on laboratory data as below:

$$\frac{R}{H_0} = \xi_0 \qquad (1)$$

for $\xi_0 \leq 2.3$ where H_0 is the significant deep water wave height and ξ_0 is the surf similarity parameter which is calculated from the deep water significant wave height and length. Based on that equation, the wave run-up was calculated with wave data at the time of image. The average wave run-up is 1.0m, ranges from single maximum run-up of 3.0m to a minimum of 0.6m and standard deviation 0.5m. After that the shoreline was being corrected to the same level i.e. the mean water level at Tokyo Port (TP-0 level). The tidal correction uses data from tidal station at Sendai Port and Ayukawa station (40km from Sendai Port). So the shoreline correction value was obtained by using calculation from wave run-up, tidal data and average beach slope (i.e. 0.11) from Kurosawa and Tanaka (2001).

Uncertainty Assessment

Several sources of error will impact the accuracy of shoreline measurement. The error that is not resolved becomes the uncertainty of measurement result. There are two types of error in the shoreline change analysis using aerial photograph i.e. error from data sources itself (aerial photo) and error from the measurement methods (Moore, 2000). Recently, the error from data source has been minimized by the development of aerial photograph technology and rectification process. The errors from this source contribute significant influence only on the small scale aerial photograph (Thieler and Danforth, 1994 in Moore, 2000).

The rectification is the process of making an image conforms to another image or any map coordinate system. The process attempted to match the points in the image to the Ground Control Points (GCP) from the mapping system. The GCP can be collected from stable points in maps, triangulation stations from government institution or field survey by using GPS technology. However, there are still some problems related to the GCP during the rectification process (Moore, 2000). Therefore, regardless of how accurately the GCP are known, the error might still remain after the rectification process.

This study only considers assessing rectification errors that become uncertainty in this measurement. As mention in previous section, the GIS program has shown the rectification error is about 6.0m. The rectification error means the average error between actual coordinates from base map and result coordinates in image. The uncertainty assessments also were carried out among the images after rectification. The photograph of May 2009 has zero tilt angles and was determine as the base image. The position coordinate of other images was checked against the base image. The assessments specially were done at three fixed position near the baseline of shoreline measurement. The results show that the error is going bigger from the south to the north. The averaged RMS error is 5.27 m in overall and conform to the error has shown by the GIS program. This rectification error is considered as uncertainty in this measurement.

Shoreline Change Analysis

In order to understand the behavior of shoreline before future analysis will be made, the measurement results will be described firstly in temporal and spatial term. In temporal term, it will be calculated the mean of shoreline position and standard deviation (σ) in every section. The results of that calculation will show the movement of shoreline during the time. The trend of shoreline movement, i.e. advance or retreat, is more interesting in the shoreline change analysis. Therefore, it will be described also the rate of change (a) every section by using simple linear regression from relationship as follows:

$$y_s = a\,t + b \qquad (2)$$

where y_s : shoreline position in a section, t : time. In spatial term, we can analyze the behavior of shoreline change on left and right side of river mouth.

Empirical Orthogonal Function (EOF) Method

The Empirical Orthogonal Function (EOF) analysis was first developed in the early 1900's. The analysis is used for extracting the dominant pattern from random data sets. In the beginning the EOF analysis are widely used in meteorology, oceanography, and other study fields. The first application on coastal morphology was done by researchers at Scripps Institute of Oceanography. Winant et al. (1975) applied this method to the analysis of beach profile data sets collected at Torrey Pines, California. Since then, this application has continued become popular specially to focus upon cross-shore variability. One of recent application on long-shore variability is described in Miller and Dean (2007), where the EOF method was applied to shoreline data sets collected from some places at United States and Australia. In EOF method, the shoreline data can be expressed as follows:

$$y(x,t) = \sum_{k=1}^{n} c_k(t).e_k(x) \qquad (3)$$

where $y(x,t)$ denotes the variability from mean shoreline ($y(x,t) = y_s(x,t) - \bar{y}(x)$, $y_s(x,t)$: the distance from baseline to shoreline, $\bar{y}(x)$: the mean shoreline), $c_k(t)$ is the temporal eigenfunction, $e_k(x)$ is the spatial eigenfunction, and n is the number of sections. The combination $c_k(t).e_k(x)$ denotes a mode of change and its variation through time. The first mode describes the most variance in the dataset and will reduce with the higher mode.

In this study, the EOF analysis was applied to the shoreline data in alongshore direction as same as research conducted by Miller and Dean (2007) and Fairley et al. (2009). The analysis was done separately between left and right side of river mouth to examine different behavior between them. The relationship between EOF results and natural parameters (i.e. wave and river discharge) was also investigated to verify physical reflection of EOF results. However, some relationship is conducted in indirect way through another parameter. The previous researches conclude that the first mode of variability reflects the cross-shore process and the second mode reflect the long shore process on shoreline movement. So the results of EOF method can be used to investigate the influence of river mouth to the surrounding beach.

RESULTS AND DISCUSSIONS

Shoreline Change Rate

Figure 3 is showing the fluctuation of shoreline position on some section at left and right side of river mouth. All graphs show same short fluctuation due to seasonal influence every year. The graphs also show long term fluctuation but in different magnitude between left and right side. On the left side, the shoreline was moving retreat from 1990 until 2001, moving advance from 2002 until 2005, and then retreat again from 2006 until 2009. The right side shows same trend but with less magnitude.

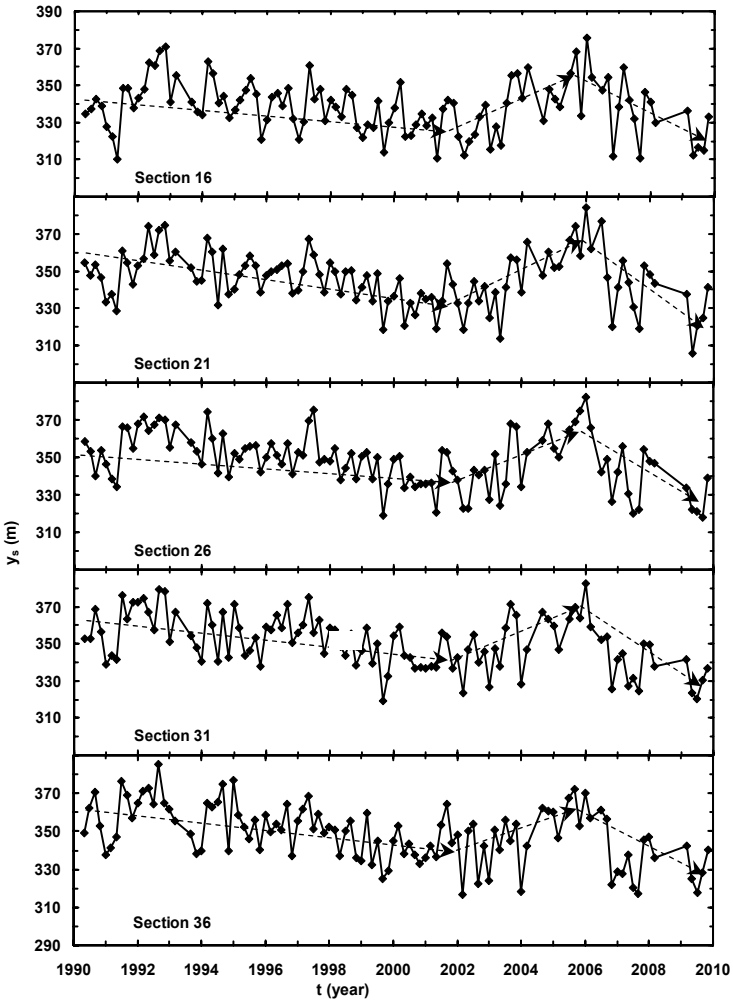

(a) left side of river mouth

Figure 3. Shoreline position from 1990 ~ 2009.

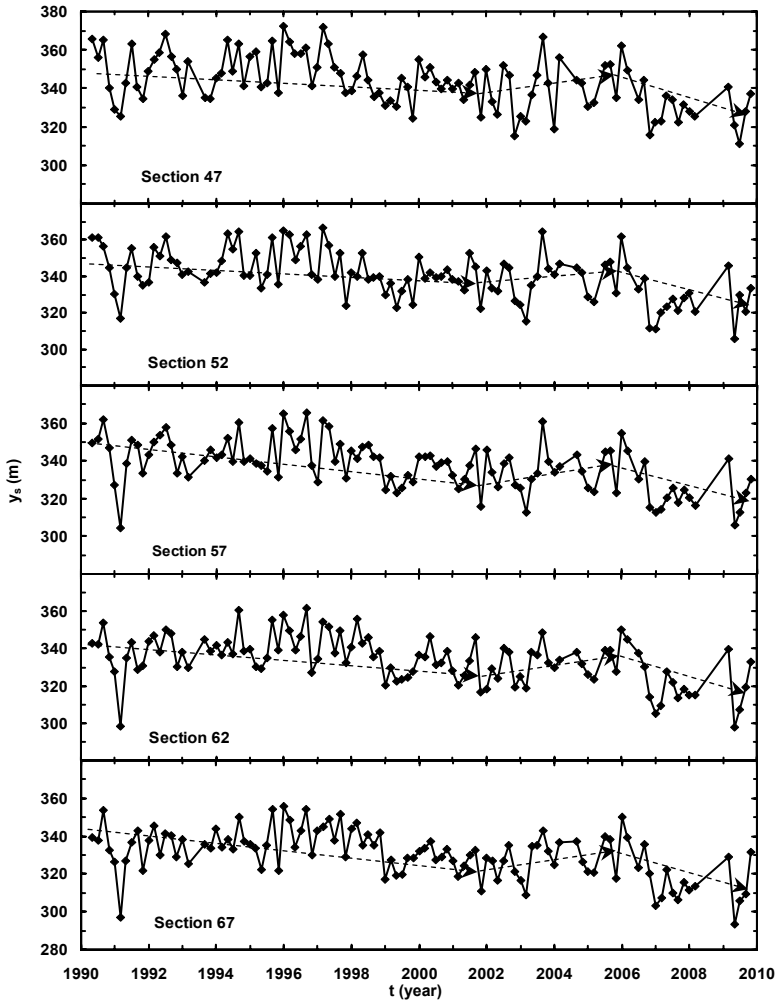

(b) right side of river mouth

Figure 3. Shoreline position from 1990 ~ 2009 (contn'd)

In Figure 4(b), it shows the mean shoreline position is steady linear increase toward river mouth on both sides. It is clearly showing the effect of river mouth to obstruct the sediment movement around it. The fluctuation of shoreline position range about 70m from minimum until maximum position on both sides. The standard deviation of fluctuation is about ± 14m on left side and ± 12m on right side as can be seen in Figure 4(c). These magnitudes are still bigger than the uncertainty ± 5.27m. Therefore, this shoreline measurement result is considered acceptable.

The calculation of shoreline change rate was performed in some time interval as indication of long term fluctuation from previous explanation. As can be seen in Figure 4(d), the shoreline on left side move retreat with rate about -1 m/yr from 1990 until 2001, move advance with rate 8 m/yr from 2002 until 2005, and then move retreat again with rate -7 m/yr. The right side of river mouth clearly show same trend but with less magnitude. These results show that the shoreline behavior of left side has more fluctuation than right side. The river mouth as source of sediment might give more influence to the left side related with the average direction of longshore sediment transport from right to left. The existence of Sendai Port breakwater on the left side might also contribute the influence in this area. The left side is like bounded by breakwater and river mouth that make high fluctuation compare with right side.

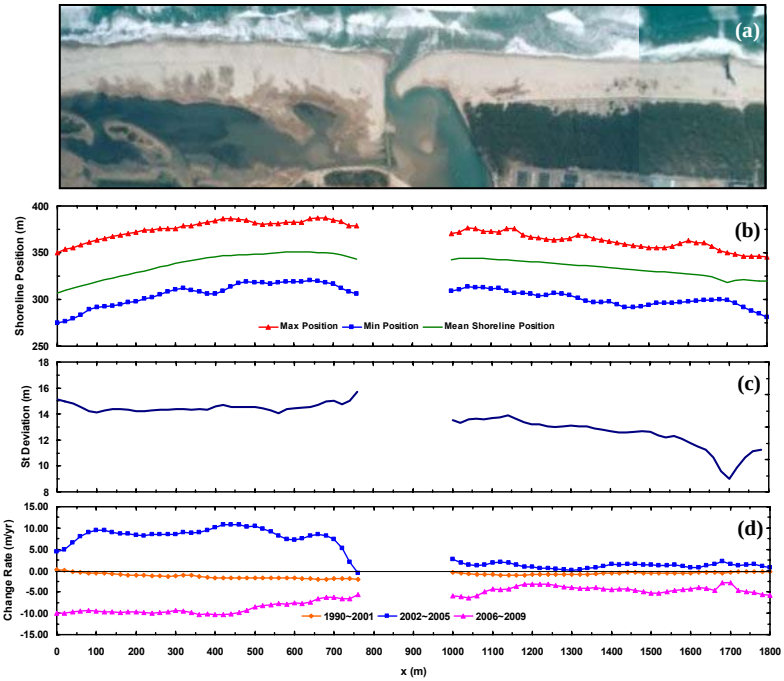

Figure 4. Shoreline change from 1990 ~ 2009.

EOF Analysis

The mode of spatial eigenfunction can be seen on Figure 5. The first mode (Fig. 5(b)) shows almost uniform shape alongshore.

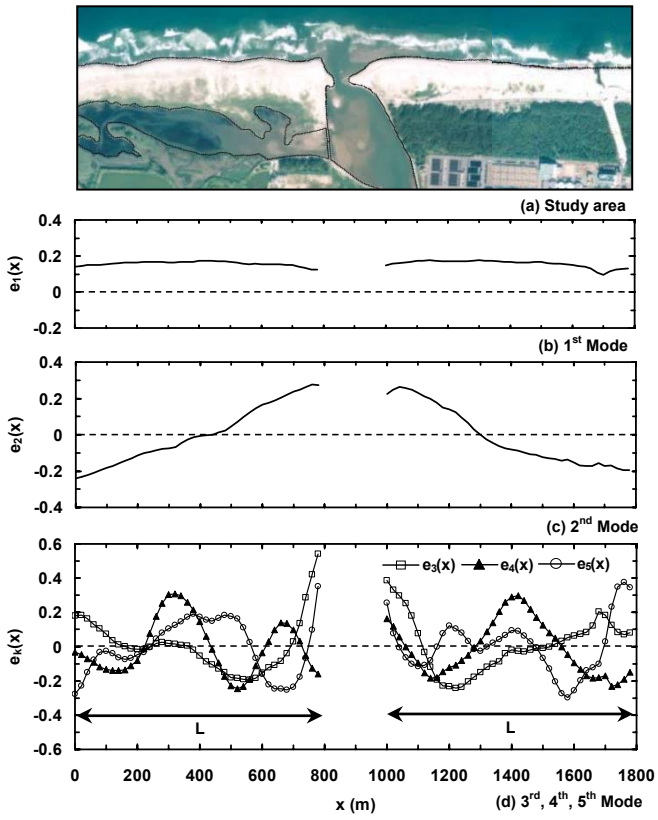

Figure 5. First five spatial eigenfunctions.

The higher modes (Figs.5(c) and (d)) show fluctuation with increasing cycles and the contribution become less and less as mentioned in Table 1. These behaviors of spatial eigenfunction seem similar to

Fourier series expansion. The first mode similar with constant term and the next modes similar with sinus-cosinus function of Fourier series. Since the length of analysis region (L) is 800 m, the wave length of second, third, fourth and fifth mode correspond to $2L$, L, $L/2$ and $L/3$, respectively.

Table 1 shows the contributions of first five eigenfunctions which have majority in the shoreline variation at each side. The first five eigenfunctions account for over 95% of the total variability. The first mode of eigenfunction described by $e_1(x)$ dominate the variability on all side. However, the first mode has less influence on left side than right side. The other way, the second mode ($e_2(x)$) has bigger influence on left side than right side. The contributions of higher modes (e_3, e_4, e_5) become much smaller and less.

Table 1. The contribution of eigenfunction modes

Data set	Contribution (%)				
	$e_1(x)$	$e_2(x)$	$e_3(x)$	$e_4(x)$	$e_5(x)$
Left side	75.1	13.4	3.4	2.1	1.8
Right side	83.5	7.0	2.4	1.7	1.3

First Mode of Variability

The first mode gives the biggest contribution to the variability of shoreline position. The left side has 75.1% and is less than right side which has 83.5%. The spatial eigenfunction show the way of shoreline change which is positively uniform alongshore between left and right side. The Figure 6 shows the associated temporal function which denotes the way of shoreline change along the time. It shows the frequent fluctuations due to seasonal change every year. In long term, the c_1 also show same behavior with shoreline change as shown in Figure 3. The trend is going minus (retreat) from 1990 until 2001, going positive (advance) from 2002 until 2005, and then going minus again from 2006 until 2009.

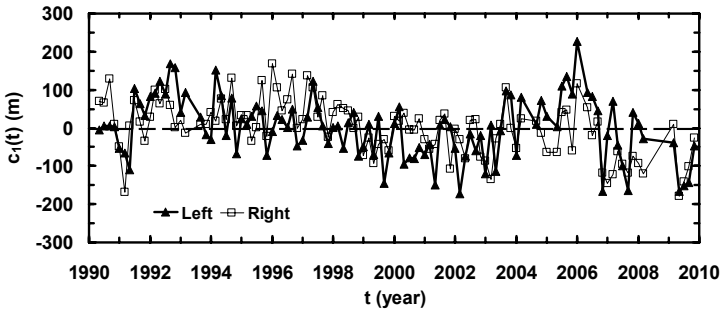

Figure 6. First mode temporal eigenfunction.

The multiplication of spatial eigenfunction and its associated temporal function will show the variability of shoreline position from average position due to first mode. Figure 7 show the result of combination of the first mode.

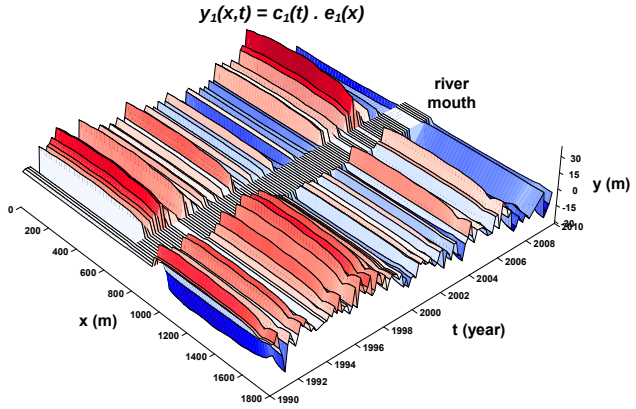

Figure 7. First mode combination of temporal eigenfunction and spatial eigenfunction.

Those combinations show uniform shoreline advancement or recession depending on the sign of temporal function. Correlate with natural process in coastal area, this condition same with beach profile

change due to seasonal change of wave condition every year. During the high waves, the beach is eroded; the eroded sediment is transported to deeper area as longshore bar and the shoreline become retreat. The sediment in longshore bar is transported back to the beach line and the shoreline become advance again when the waves become calm again. In this situation there are uniform movements of shoreline in cross-shore direction. It means the correlation of first mode temporal function between left and right side should be in positive relation. Figure 8 show the correlation of c_1 between left and right side with correlation coefficient (r) is 0.52 in 95% confidence interval. It may conclude that the first mode of variability from EOF analysis reflect the cross-shore movement of shoreline.

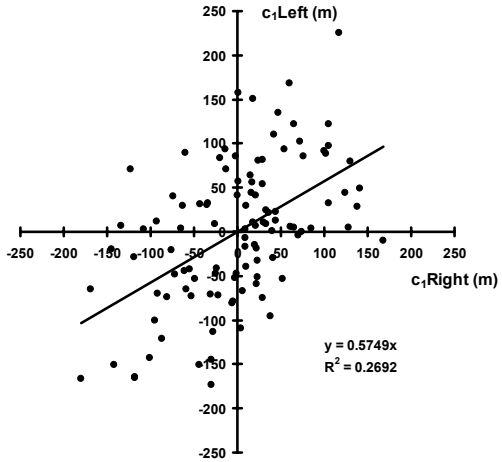

Figure 8. Relationship of first mode temporal eigenfunction between left and right side.

In order to correlate the result of EOF analysis with natural process, we examine the relationship between temporal function and natural parameters such as wave height, wave length and river discharge. However, we make correlation indirectly, for temporal function we calculate the gradient of c_1 ($=\Delta c_1/\Delta t$) which more appropriate to express the condition of beach. If the gradient value is positive means in accretion condition and negative means erosion. Same as temporal function, we also calculate the natural parameters in terms of Cs parameter from Sunamura and Horikawa (1974) which also express the condition of beach in accretion or erosion stage.

$$Cs = \frac{Ho}{Lo}(\tan\beta)^{0.27}\left(\frac{d}{Lo}\right)^{-0.67} \qquad (4)$$

where H_0 is deep water wave height, L_0 is deep water wave length, β is beach slope and d is sediment size. If the Cs value become high means in erosion condition and low means accretion condition. To make same comparison in terms of time with temporal function, we calculate the average value of Cs in 2 months between consecutive images. The expectation is $\Delta c_1/\Delta t$ has negative correlation with Cs average and is shown in Figure 9 with correlation coefficient $r = 0.22$ in confidence interval 95%.

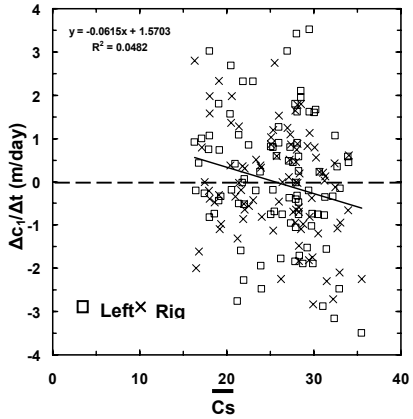

Figure 9. Relationship between *Cs* average and Gradient c_1.

Second Mode of Variability

The second mode of spatial eigenfunction has one nodal point on both sides. In this mode the left side get bigger influence (13.4%) than right side (7.0%). The Figure 10 shows the associated temporal functions which have smaller fluctuation than the first mode. The second mode does not show long term fluctuation as same as the first mode. Figure 11 shows the combination of spatial eigenfunction and temporal function of second mode. It shows the four types of combination which is depend on the value of temporal eigenfunction.

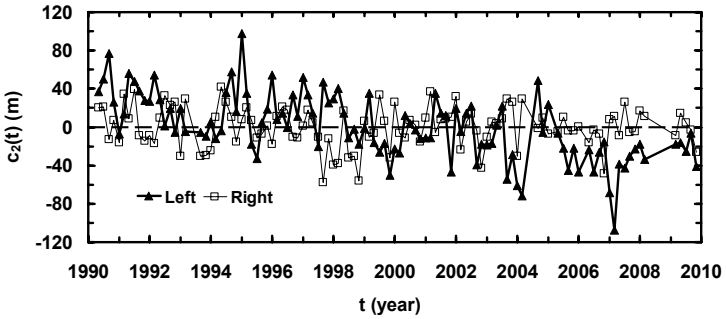

Figure 10. Second mode temporal eigenfunction.

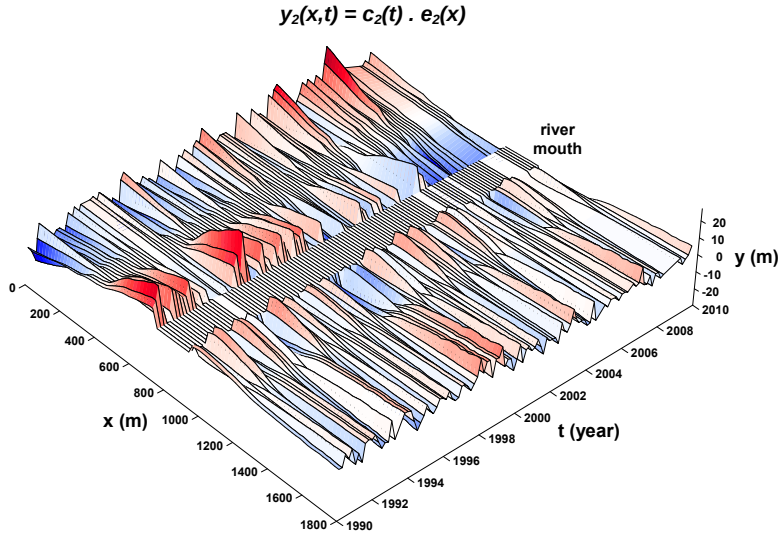

Figure 11. Second mode combination of temporal eigenfunction and spatial eigenfunction.

Figure 12 shows clearly the four combination possibility in second mode. The shoreline will become opposite slope (positive-negative or negative-positive) between left and right side as shown in Figure 12(b) or Figure 12(c) if the condition of temporal function on both side in same sign (+/+ or -/-). On the contrary, the shoreline become same slope (positive-positive or negative-negative) between left and right side as shown in Figure 12(a) or Figure 12(d) if the condition of temporal function on both side in opposite sign (+/- or -/+). When the combination in same slope, this condition reflect the influence of river mouth to interrupt the longshore sediment transport that making deposition on one side and erosion on another side as same as the influence of jetty structure. Therefore, the expectation relationship of second mode temporal function between left and right side is negative correlation.

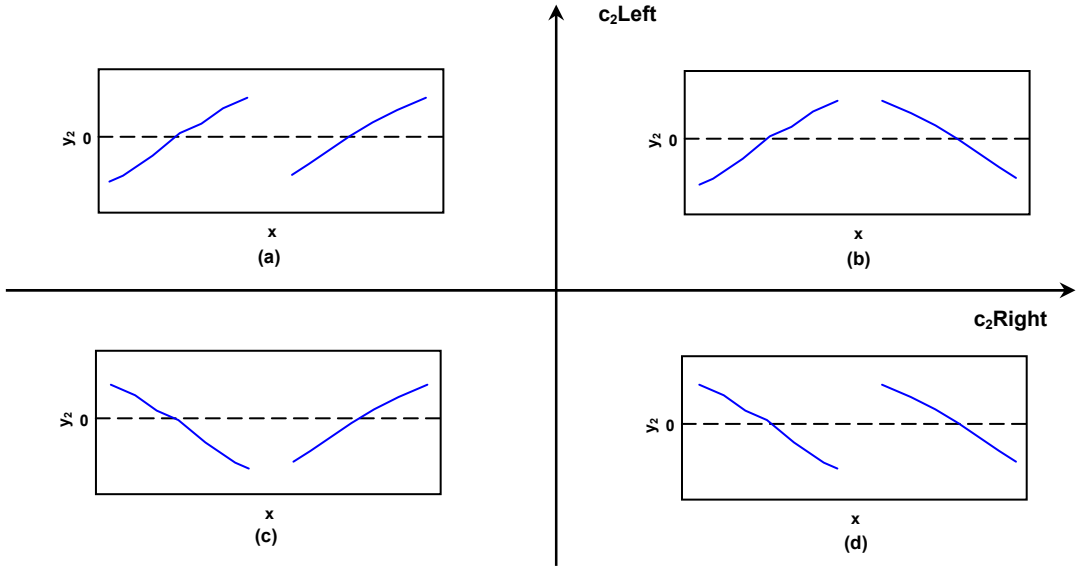

Figure 12. Four combination possibility in second mode.

However, the negative correlation is weak as can be seen in Figure 13. The weak correlation might be influenced by the event of high discharge ($Q > 10\ m^3/s$). Figure 14 shows the plotting of second mode temporal eigenfunction and river discharge from 1990 until 2003. The vertical grey line indicates the river discharge bigger than $10m^3/s$. It shows relatively many high discharges occur in the same positive c_2 value on both sides. It is indicated also in Figure 13 that many high discharges are plotted in first quadrant. That makes the shoreline shape as same as depicted in Figure 12(b). It can be explained that the river supply more sediment to the beach and collected on both side of river mouth during the high discharge. Other data which have negative correlation clearly shows the influence of river mouth on longshore sediment transport even without the existing of jetty structure.

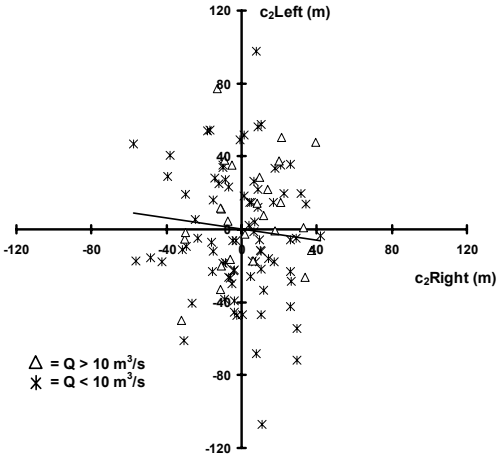

Figure 13. Correlation of second mode temporal eigenfunction between left and right side.

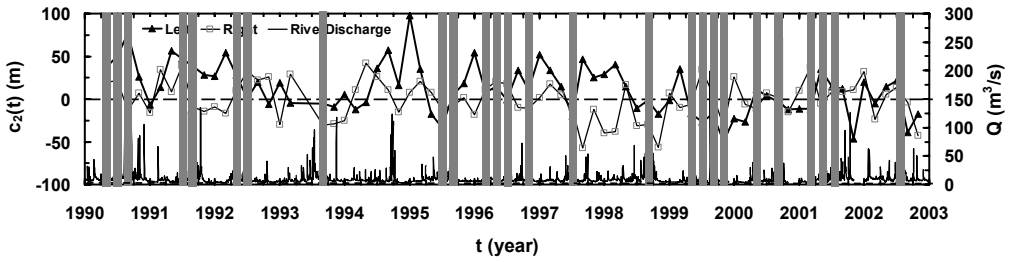

Figure 14. Relationship of second mode temporal eigenfunction and river discharge.

Third, Fourth and Fifth Mode of Variability

The spatial eigenfunction of mode 3, 4 and 5 have more nodal points on both sides. The contribution and temporal function of these modes have less magnitude than previous mode. These three modes might reflect the existence of beach cusp. We examine the correlation between the temporal function of these modes with wave parameters K_* defined by the following equation (Sunamura, 1986).

$$K_* = \frac{\overline{H_b}^2}{g\,\overline{T}^2\,d} \tag{5}$$

where $\overline{H_b}$ is the daily average breaking wave height, $\overline{T}$ is daily average wave period and g is gravity acceleration. The beach cusp will appear during the process of beach change when the K_* value between 5 and 20. In that time, we expected the absolute value of temporal function (c_k) become bigger.

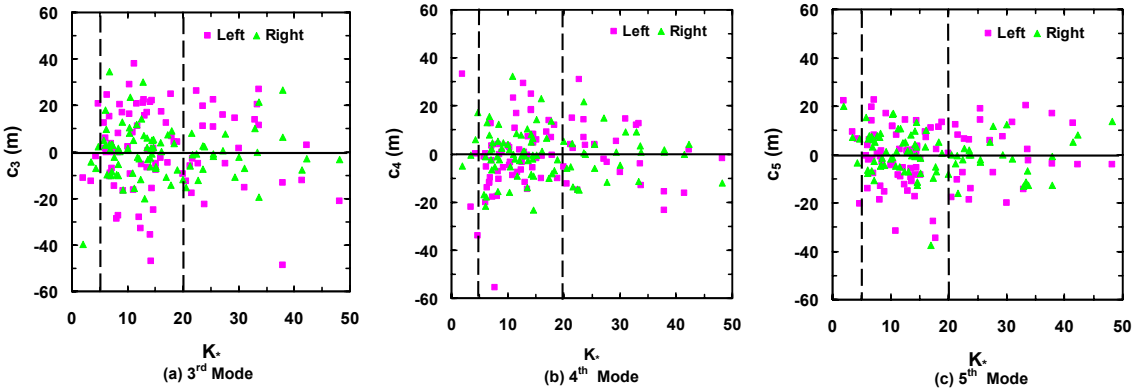

Figure 15. Correlation of 3rd, 4th, 5th mode temporal eigenfunction with K_*.

From Figure 15 we can see most of the temporal function occupy the region between 5 and 20 of K_*. We may conclude that the Mode 3, 4 and 5 reflect the existence of beach cusp.

CONCLUSION

The shoreline behavior analysis around river mouth has been performed in this study by utilizing aerial photograph which have been taken for 20 years. The analysis on frequent aerial photograph has exposed clearly the shoreline behavior around the Nanakita River mouth. The shoreline on both side of river mouth has same short time fluctuation which is influenced by annual seasonal change. However, the left side have higher fluctuation than right side in long term scale. The shoreline on left side has been moving more dynamically than right side of river mouth. The situation of left side shoreline is like bounded by Sendai Port breakwater and Nanakita River mouth. That situation might cause the dynamic behavior in that area.

The results of EOF analysis show that the first mode of eigenfunction reflects the cross-shore movement of shoreline. Then the shoreline change around the Nanakita River mouth is dominated by cross-shore movement with contribution of first mode around 75%. The second mode of eigenfunction reflects the longshore movement of shoreline. This mode also shows the influence of river mouth to the longshore sediment transport by different response of shoreline between left and right side of river mouth. The shoreline change around the Nanakita River mouth is influenced by longshore movement only around 10% from the contribution of second mode. The third, fourth and fifth mode of eigenfunction reflect the existence of beach cusp.

ACKNOWLEDGMENTS

This study was financially supported by the Grant-in-Aid for Scientific Research from JSPS (No. 21360230). This study is also part of doctoral study of first author at Tohoku University which is

supported by the Ministry of National Education, the Republic of Indonesia. The authors would like to gratefully appreciate these financial supports.

REFERENCES

Boak E.B., and I.L. Turner. 2005. Shoreline definition and detection: a review, *Journal of Coastal Research*, Vol. 21, No. 4, pp. 688–703.

Camfield F.E., and A. Morang. 1996. Defining and interpreting shoreline change, *Ocean & Coastal Management*, Vol. 32, No. 3, pp. 129-151.

Crowell M., S.P. Leatherman, and M.K. Buckley. 1991. Historical shoreline change: error analysis and mapping accuracy, *Journal of Coastal Research,* Vol. 7, No. 3, pp. 839-852.

Dibajnia M., R.B. Nairn, and P. Ross. 2004. Analysis of longterm sand accumulation at a harbor using 2DH numerical simulation, *Coastal Engineering,* 51, pp. 863-882.

Fairley I., M. Davidson, K. Kingston, T. Dolphin, and R. Phillips. 2009. Empirical orthogonal function analysis of shoreline changes behind two different designs of detached breakwaters, *Coastal Engineering*, Vol.56, pp.1097-1108.

Hanslow D.J. 2007. Beach erosion trend measurement : a comparison of trend indicators, *Journal of Coastal Research*, Special Issue 50, pp. 588-593.

Hoeke R.K., G.A. Zarillo, and M. Synder. 2001. A GIS based tool for extracting shoreline position from aerial imagery (BeachTools), *Coastal and Hydraulics Engineering Technical Note*, CHETN-IV-37, U.S. Army Corps Engineer Research and Development Center, Vicksburg, MS.

Hunt I.A. 1959. Design of seawalls and breakwaters, *Journal of Waterway and Harbors Division*, ASCE, 85(3), pp. 123-152.

Kang H.W., and H. Tanaka. 2004. Monitoring of long-term shoreline evolution on Sendai coast, *Proceedings of the 4th Congress of Environmental Hydraulics and the 14th Congress of APD-IAHR Congress*, pp.1101-1107.

Khang T.T., and H. Tanaka. 2007. Effect of river mouth terrace to the continuous longshore sediment transport on Sendai coast, *Journal of Coastal Research*, Special Issue 50, pp. 874-878.

Kraus N.C., and J.D. Rosati. 1997. Interpretation of shoreline position data for coastal engineering analysis, *Coastal Engineering Technical Note*, CETN-II-39, U.S. Army Corps Engineer Coastal Hydraulic Laboratory.

Kuroiwa M., T. Kuchiish, K. Kato, S. Sunagawa, and Y. Matsubara. 2008. Applicability of coastal area model to morphodynamics around river mouth, *Proceedings of 31th International Conference on Coastal Engineering*, ASCE, pp. 2218-2230.

Kurosawa T., and H. Tanaka. 2001. A study of detection of shoreline position with aerial photographs, *Proceedings of Coastal Engineering*, Vol. 48, Japan Society of Civil Engineer, pp. 586–590 (in Japanese).

Miller J.K., and R.G. Dean. 2007. Shoreline variability via empirical orthogonal function analysis: Part 1 temporal and spatial characteristics, *Coastal Engineering*, 54 (2), pp. 111-131.

Moore L.J. 2000. Shoreline mapping techniques, *Journal of Coastal Research*, Vol. 16, No. 1, pp. 111-124.

Srivihok P., and H. Tanaka. 2004. Analysis of river mouth behavior change by using aerial photographs, *Annual Journal of Hydraulic Engineering*, Vol. 48, Japan Society of Civil Engineer, pp. 733-738.

Sunamura T., and K. Horikawa. 1974. Two-dimensional beach transformation due to waves, *Proceedings of 14th International Conference on Coastal Engineering*, ASCE, pp. 920-938.

Sunamura T. 1986. A parameter for cross-shore sediment transport direction and its application to beach erosion/accretion problem, *Annual Report*, Inst. Geosci., Univ. Tsukuba, No.12, pp. 52-54.

Uzaki K., and Y. Kuriyama. 2007. Numerical and field study of sediment budgets on an intertidal flat at the mouth of the Shirakawa River, *Proceedings of 5th River, Coastal and Estuarine Morphodynamics : RCEM 2007*, IAHR, pp. 427-434.

Winant C.D., D.L. Inman, and C.E. Nordstorm. 1975. Description of seasonal beach changes using empirical eigenfunctions, *Journal of Geophysical Research*, 80 (15), pp. 1979-1986.